

Synthesis, Characterisation of Novel Polyaniline Nanomaterials and Application in Amperometric Biosensors

I. Michira, R. Akinyeye, V. Somerset, M. J. Klink, M. Sekota, A. Al-Ahmed, P. G. L. Baker, E. Iwuoha*

Summary: Anthracene sulfonic acid doped polyaniline nanomaterials were prepared through the chemical oxidative polymerisation process. Ammonium peroxydisulfate (APS) was employed as oxidant. Scanning electron microscopy (SEM) results show the resultant polyaniline (PANI) materials exhibited nanofibrillar morphology with diameter sizes less than 300 nm. Using the nanofibrillar PANI, amperometric biosensors for H_2O_2 and erythromycin were constructed through the drop-coating technique. Anthracene sulfonic acid (ASA) doped PANI and the test enzymes horseradish peroxidase, (HRP), or cytochrome P_{450} 3A4, (CYP_{450} 3A4) were mixed in phosphate buffer solution before drop coating onto the electrode. The resultant biosensors displayed typical Michaelis-Menten behaviour. The apparent Michaelis-Menten constant obtained was 0.18 ± 0.01 mM and 0.80 ± 0.02 $\mu\text{M L}^{-1}$ for the peroxide and erythromycin biosensor respectively. The sensitivity for the peroxide sensor was $3.3 \times 10^{-3} \text{ A} \cdot \text{cm}^{-2} \cdot \text{mM}^{-1}$, and the detection limit was found to be 1.2×10^{-2} mM respectively. Similarly, the sensitivity for the erythromycin sensor was in the same order at $1.57 \times 10^{-3} \text{ A} \cdot \text{cm}^{-2} \cdot \text{mM}^{-1}$ and detection limit was found to be 7.58×10^{-2} μM .

Keywords: doped polyaniline; electroactive; enzymes; nanocomposites; synthesis

Introduction

The recent tremendous interest in nanomaterials is due to their fascinating and useful characteristics with a promisingly great application potential.^[1–4] With grain sizes in the order of a nanometer, nanomaterials exhibit excellent mechanical, catalytic, magnetic and optical properties. The recent great interest in polyaniline (PANI) fabrication relates to its good environmental stability and the fact that its electrical properties can easily be modified through dopant inclusion/exclusion principles. PANI is finding use in the fabrication of electromagnetic interference shielding materials,

and in broadband microwave adsorbing materials.^[5] It has also merited applications in many other fields including; biosensor technology, electrochromic devices, energy storage systems and anticorrosion materials. However, its large-scale applicability has been encumbered by its poor thermal stability and difficult processability.

Doped PANi is hard, brittle and insoluble in common organic solvents making its large-scale processability difficult. Since the insolubility/infusibility of PANi is related to its rigid π - π^* conjugation system several strategies employed to overcome both PANi organic and inorganic insolubility target this system. Introduction of substituents^[6–8] on the aromatic ring or imine nitrogen, copolymerization with aliphatic monomers,^[2] preparation of PANi blends / composites with other convectional polymers^[9–11] have led to more soluble PANi.

Sensor Research Laboratory, Department of Chemistry, University of the Western Cape, Belville, 7535, Cape Town South Africa
E-mail: eiwuoha@uwc.ac.za

Preparation of PANi colloidal dispersions through; polymerisation of aniline monomers in a micellar, emulsion, reversed micro-emulsion media or in the presence of polymeric stabilizers have yielded colloidally stable PANi with submicrometer/nanometer sized particles.^[2]

In general PANi is produced through the chemical and the electrosynthetic routes. The chemical synthesis entails the oxidative polymerisation of the requisite monomers in an acidic media using strong oxidants^[12] in presence or absence of templates. If present in the polymerisation bath, templates avail nanoscopic void spaces for structurally molding the morphology of the resultant PANi into defined nanoshapes. Polycarbonate track-etched membranes, anodic aluminium oxide and aluminosilicate have been used as templates for nanometer sized PANi. Surfactant templates however, have recently generated a lot of interest. This is because surfactant templates package their structure directing role with the ability to solubilize and stabilize the resultant PANi colloids besides acting as dopants. Sodium dodecyl benzene sulfonic acid (DBSA), sodium dodecyl sulfonic acid (SDS) amongst others have been used.^[13]

Use of surfactant templates have resulted in diverse PANi morphology. For instance, DBSA-doped PANi was highly agglomerated making its morphology difficult to identify.^[2] In another instance, pure PANi-DBSA film displayed the formation of microtubules.^[14] Several other authors have reported formation of nanotubular PANi.^[15–17] It appears several factors including surfactant (dopant) to monomer ratios play a critical role in determining the morphology of the resultant PANi.

Besides processability improvement, nanosized PANi shows improved polymer performance in many convectional applications involving polymer interaction with the environment. Faster and more responsive sensors based on PANi nano-particles have been reported. The ability of PANi to immobilize and provide direct electrical communication between the enzyme and

electrode in amperometric biosensors has been demonstrated.^[18,19] By delocalizing redox charges over a series of conducting polymer groups, conducting polymers (including PANi) can act as self-contained electron transfer mediators.^[19]

In this study, the synthesis of a novel dopant anthracene sulfonic acid (ASA) and use it to prepare a new material, anthracene sulfonic acid doped polyaniline (PANi-ASA). Structural (UV-Vis and FTIR spectroscopy) and electrochemical (cyclic voltammetry) characterisation is used to probe the conductivity and electroactivity nature of the polymer. The ASA-doped PANi is then used in the construction of amperometric biosensors for hydrogen peroxide and erythromycin detection.

The determination of H₂O₂ and other organic peroxides is of practical importance in clinical, environmental, industrial and many other fields. The current H₂O₂ assay techniques based on volumetric, colorimetric and chemiluminescence analysis are complex, time consuming, and are prone to interferences.^[20] Polyaniline based peroxide sensors are easily fabricated and combine the exquisite selectivity of horseradish peroxidase (HRP) with the excellent PANi stability to produce sensors with high sensitivity. Also the simultaneous electro-deposition of the polymer together with the biomolecule incorporation allows for the control of the spatial distribution of the immobilized protein, control of film thickness and enzyme activity and can be manipulated to produce sensors with excellent performance.^[18,20] Several polyaniline based peroxide sensors have been reported.^[18–20]

With the onset of 'polypharmacy' – the simultaneous prescription of more than one drug to treat one or more conditions in a single patient- drug to drug interactions have been cited as one of the major causes of hospitalization/death.^[21] Besides, such interactions can increase/lower the efficacy of the other drugs calling for dosage adjustment. CYP3A4 is one of the haem-thiolato enzymes generally referred to as the cytochrome P₄₅₀ enzymes. It is the

major enzyme involved in the phase-1-biotransformation of xenobiotics.^[22] Through catalyzing hydroxylations, epoxidations, N-dealkylations, O-dealkylations reactions of xenobiotics, this monooxygenase enzyme can attach a conjugate bond to the drug rendering it pharmacologically inactive and eliminable. It has been shown that CYP 3A4 catalyses the N-demethylation of erythromycin.^[22] Erythromycin is a macrolide antibiotic, which has antimicrobial spectrum similar to that of penicillin.^[23] It is used to treat various conditions including respiratory tract infections. It has been found that the simultaneous administration of erythromycin with other drugs such as verapamil and diltiazem can lead to fatal drug-to-drug interactions.^[23]

Experimental Part

Materials and Pre-treatment

Anthracene sulfonic acid was synthesized in-house. The aniline monomer purchased from Fluka, was doubly distilled under reduced pressure before use. Dimethyl sulfoxide (DMSO), methanol, diethylether, ammonium peroxydisulfate (APS) and hydrochloric acid (HCl), bovine serum albumin and gluteraldehyde (50% w/v in water) were purchased from Fluka, (Cape Town, South Africa). The gluteraldehyde was diluted with distilled water to give a 2.5 % solution before use. The KBR salt (Aldrich), was oven dried at 80 °C for 2 h before use. AnalaR grade anhydrous disodium hydrogen phosphate and AnalaR grade potassium dihydrogen phosphate monohydrate were products of Aldrich, Cape Town, South Africa. The anhydrous salts were dried for 3 h at 110 °C and cooled in a dessicator before use for buffer preparation. Hydrogen peroxide (30%) was a product of Sigma Aldrich, Cape Town, South Africa. Horseradish peroxidase (EC.1.11.1.7) type II, 200 units/mg salt-free powder obtained from Sigma (CapeTown, South Africa) was used for the H₂O₂ biosensor preparation.

Purified cytochrome P450_{3A4} (MW 45–60 kDa) isozyme, human recombinant containing >80 pmole cytochrome P450 / mg protein was used. The CYP3A4 and erythromycin (997 µg/mg) which was used as substrate were purchased from Sigma Adrich, Cape Town, South Africa.

Instrumentation

All electrochemical measurements were carried out using a BAS 50W electrochemical workstation from BioAnalytical Systems (BAS), Lafayette, Illinois, USA. All pH measurements were done using HANNA Instruments microprocessor pH meter. The UV-Vis absorbance experiments were performed with UV/Vis 920 Spectrometer (GBC Scientific Instruments, Australia). FTIR measurements were performed using Perkin Elmer Paragon 1000 PC FTIR, in the range 400–4000 cm⁻¹ wave numbers. Scanning electron microscopy (SEM) was carried out using a Hitachi X-650 Scanning Electron Microanalyser with an operating voltage window of 5–40 kV. Specimens for SEM analysis were sprinkled on to aluminium stubs and coated with conducting glue before spraying with a thin layer of gold for 4 min prior to viewing.

Synthesis of Anthracene Sulfonic Acid

A three-necked distillation flask that has a separating funnel, a thermometer and a mechanical stirrer was used for the synthesis. 2 g of anthracene were heated through an open-air bath until it melted. To the molten anthracene, 3.73 g of 30% fuming sulfuric acid were added and the mixture was stirred continuously at 160 ± 5 °C. The resultant solution was poured into 20 mL ice-cold water and half neutralized with 4 g NaHCO₃. The resultant solution was then brought to boiling and saturated with NaCl. Recrystallization in 10% NaCl yielded sodium anthracene sulfonate, a white crystalline and highly deliquescent salt. The salt was dried in an oven at 80 °C. The properties of the salts are: yield 1.82 g (65%), FTIR, (KBr), bands at 1040 cm⁻¹ and 1020 cm⁻¹ and 505 cm⁻¹ due to -SO₃H group indicative of successful

sulfonation of anthracene. Hydrolysis of the sodium anthracene sulfonate yielded anthracene sulfonic acid. (1 M ASA, pH = 0.56).

Synthesis of Structurally Modulated PANi

2×10^{-3} mol of anthracene sulfonic acid and 4×10^{-3} mol aniline were dispersed in 20 mL distilled water under continuous magnetic stirring. The temperature of the mixture was slowly raised and held at between 50–60 °C, followed by cooling in an ice-bath (0–5 °C) under continuous stirring. 4×10^{-3} mol of pre-cooled ammonium persulfate in 5 mL distilled water was added drop-wise to the reaction mixture. Vigorous stirring continued for the next 24 h during which the light yellow solution darkened to an emerald colour and later to dark green characteristic of doped PANi. The resultant colloidal suspension was allowed to stand for another 12 h. Vacuum filtration of the product was followed by thorough washing with distilled water, methanol and diethyl ether respectively. The polymer pastes were vacuum dried for 24 h prior to characterization.

Electrochemical Procedures

Cyclic voltammetry was carried out in a 5 mL electrochemical cell with a Ag/AgCl (3 M NaCl type) and a platinum wire as reference and auxiliary electrodes respectively. A Farady cage (BAS C2) was used for all the experiments. The platinum working electrode (disc formatted type) with a diameter of 1.77×10^{-2} cm² was obtained from BAS. Prior to use, the platinum disc electrode was cleaned by polishing with 1, 0.3 and 0.03 μm alumina slurries on polishing pads (Buehler, IL, USA) respectively and then rinsed thoroughly with de-ionised water after each polishing step. The platinum wire counter electrode was flame-cleaned before use. The cell, consisting of 0.05 g polymer per 1 mL 0.1 M HCl solution was purged with analytical grade argon for 10 min prior to characterization and an argon (Afrox, SA) blanket maintained thereafter. The cell contents were subjected to 20 cycles of potential cycling between –400 mV and

+1100 mV during which there was a steady and reproducible voltammogram and a thin film formed on the electrode. Electrochemical characterization measurements were then achieved by cycling the potential in the same potential window but with varying sweep rates (0–50 mV/s).

Immobilization of Biomolecules

The platinum electrode was pretreated as previously described and then ultrasonically washed in water and ethanol for about five minutes. The PANi/HRP biosensor for electrode drop-coating was prepared by dissolving 0.2 mg HRP in 100 μL 0.05 M phosphate buffer, pH 7.0. To this enzyme solution, 3 mg of PANi/ASA powder and 0.2 mg bovine serum albumin (BSA) was stirred in followed by the addition of 2 μL of gluteraldehyde (2.5%). Finally a 3 μL aliquot of the resultant mixture was dropped on to a platinum micro-electrode (0.0177 cm²) and let to dry in the air for 2 h. The above procedure was repeated in the preparation of the PANi/CYP biosensor except in this case the enzyme concentration was 14.4 μM^L⁻¹ and the concentration of the phosphate buffer used was 0.1 M, pH 7.4, and contained 100 mM KCl.

The electrocatalytic behaviour of the PANi/ASA/HRP and the PANi/ASA/CYP3A4 biosensors was studied using Bioanalytical System (BAS) CV-50W on the potentiodynamic mode. CVs were recorded (at 5 mV/s in a potential range of 400–800 mV) with and without H₂O₂ (or erythromycin) in phosphate buffer 7.0 for H₂O₂ and phosphate buffer saline (PBS, pH 7.4, 100 mM KCL) for erythromycin. A platinum counter and a Ag/AgCl (3 M NaCl) reference electrode were used. Test solutions consisted of small portions of 0.01 M H₂O₂ (in distilled water) or 0.0005 M erythromycin (in PBS) respectively.

Results and Discussion

Scanning Electron Microscopy Results

Scanning electron microscopy (SEM) showed that the ASA anionic dopant

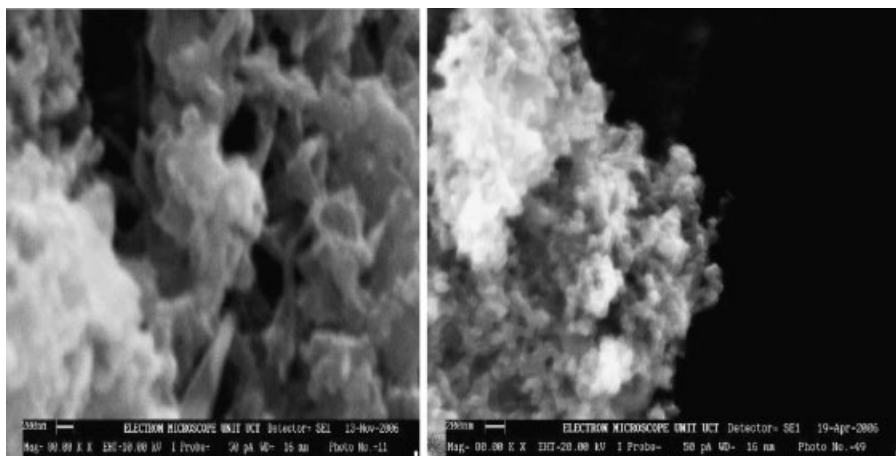


Figure 1.

SEM micrographs of chemically synthesized anthracene sulfonic acid doped PANi. The aniline to anthracene sulfonic acid ratio was 1: 0.5.

modulated the morphology of the resultant PANi into nanofibrils (Figure 1). These nanofibrils exhibited diameter sizes mainly less than 200 nm. It is proposed that the ASA micelles or the ASA/ polymer clusters formed, guided the formation of fibrillar morphology.^[24] Similar structures were reported for camphor sulfonic acid doped PANi.^[24,25] The SEM morphology obtained indicates the presence of polymer over-growth leading to agglomeration.

Spectroscopical Characterisation

The nano-fibrillar ASA-doped PANi was subjected to further structural characterization to determine its conducting state. The success of these techniques is based on the fact that doping structurally modulates the structure of the resultant PANi leading to the emergence of new bands in its spectrum. Because of doping, new electronic energy levels are introduced between the valence and conducting band of the polymer in the gap.^[26] As a result and depending on the doping level, two or three transitions can take place inside the band gap a phenomenon associated with increased polymer conductivity with doping. Intra-gap transitions introduce charge carriers within the polymer backbone hence boosting polymer conductivity.

Under normal circumstances, the UV-Vis spectrum of undoped PANi (Figure 2) exhibits two characteristic bands; a band at ca. 300 nm (peak a, Figure 2) due to $\pi-\pi^*$ transitions of the benzoid ring, and another at ca. 600 nm (peak b, Figure 2.) due to $\pi-\pi^*$ transitions of the quinonoid structure.^[17,27]

Figure 2 also represents the spectrum of ASA-doped PANi as compared to that of pristine PANi. The PANi-ASA nanofibrils were converted to the emeraldine base form by dedoping with 10% $\text{NH}_3\cdot\text{H}_2\text{O}$ for 12 h.

This figure indicates that the spectrum of doped PANi is marked by the appearance of two new bands. The band at 420 nm is assigned to an intermediate state formed during the electro-oxidation of the poly-leucoemeraldine form of PANi and that involves three sub-band gap transitions.^[26] This absorption band is due to the charged para-coupled phenyl structures corresponding to phenyl excitons or polarons.^[28] The band at 850 nm may be due to defects in the polymer.^[29] The existence of polaron defects within the PANi backbone is indicative of its conducting nature. The diminished exciton band at 600 nm for doped PANi is a sign of complete doping.^[30]

The FTIR spectrum of ASA-doped PANi composite is shown in Figure 3.

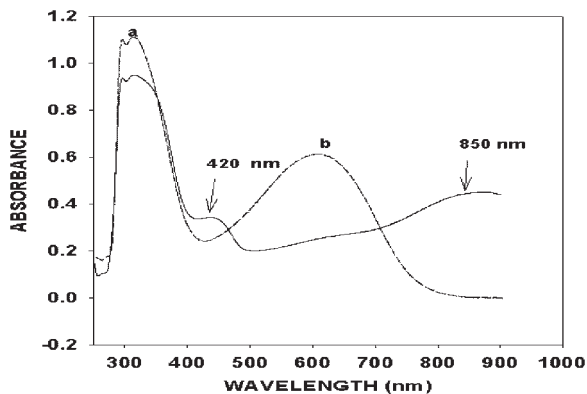


Figure 2.

UV-Vis results of undoped and doped PANi. Anthracene sulfonic acid was used as dopant. Undoped PANi was characterized by two peaks at 320 nm (peak a) and at 600 nm (peak b).

The peaks at 1580 cm^{-1} ($-\text{C}=\text{C}-$, quinoid ring), 1495 cm^{-1} ($-\text{C}=\text{C}-$, benzoid ring), $1200\text{--}1300$ (B-C-N stretching mode) and the electronic-like absorption mode of $\text{N}=\text{Q}=\text{N}$ stretching vibrations at 1100 are in close resemblance to those published in literature.^[30,31] The peaks at 1040 and 505 cm^{-1} correspond to the stretching and bending vibrations of the $-\text{SO}_3\text{H}$ functional group.^[17] The occurrence of these peaks in the PANi/ASA spectrum polymer was successfully doped.

EDX results for the ASA/PANi nanocomposites exhibited % atomic composi-

tion of 92.99 C, 2.16 O, 3.32 S, and 1.53 Cl. This result correlates the FTIR findings that the PANi was successfully doped.

Voltammetric Measurements

Figure 4, represents the cyclic voltammogram (CV) of the anthracene sulfonic acid modulated PANi recorded 0.1 M HCl solution. The CV was recorded in the potentiodynamic mode with potential sweeping between -400 mV and $+1100\text{ mV}$ between 10 and 50 mV/s scan rate. All potential measurements were done with respect to a Ag/AgCl (3 M NaCl type)

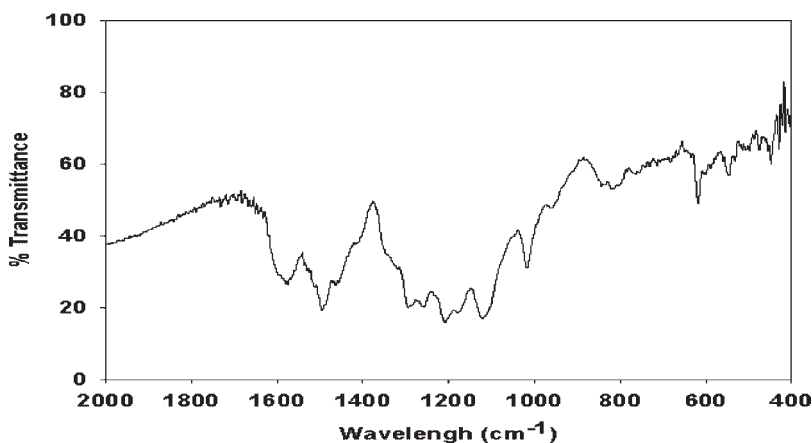


Figure 3.

FTIR spectra of anthracene sulfonic doped PANi recorded through KBr disc method.

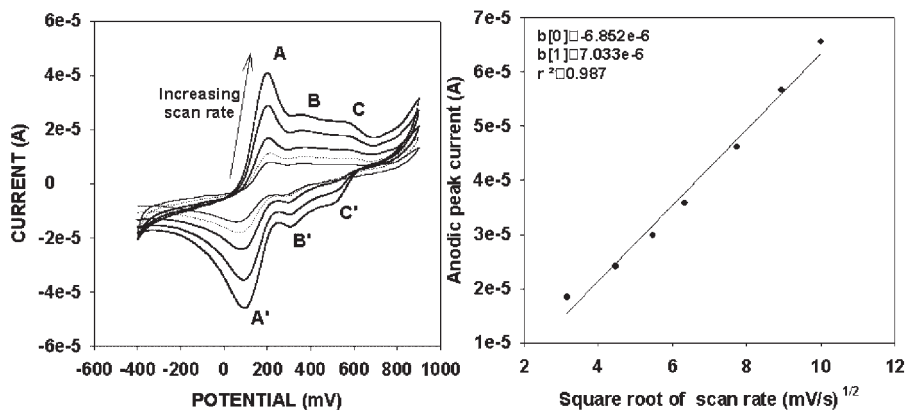


Figure 4.

Cyclic Voltammogram of ASA-doped PANi in 0.1 M HCl between 10–50 mV/s on a platinum micro-electrode. The linear graph represents the Randles-Sevcik showing peak A current dependence on square root of scan rate.

reference electrode. The CV displays well defined oxidation-reduction responses indicating that the PANi/ASA nanocomposite is electroactive.^[32] The first redox process A/A', with a formal potential, ($E^{(0)}$) of 190 mV represents the polyleucoemeraldine/emeraldine salt transition (PNB/ES).

The second redox couple B/B' observed at $E_{pa} = 555$ mV and $E_{pc} = 496$ mV is due to the degradation products of over-oxidized PANi.^[33] Several authors assign this reversible couple ($\Delta E_p = 59$ mV) to the redox reactions of the degradation products hydroquinone to quinone.^[34] Peaks B/B' could also be due to defects in the linear structure of the polymer.^[35] The third redox couple (C/C'), represents the poly-emeraldine salt (ES)/ polypernigraniline (PNB) transition.^[36] The oxidation of this polysemiquinone radical cation (ES) form of PANi (redox couple (C/C')) occurred at E^0 700 mV. The formal potentials obtained in this study are in unison with literature values reported for doped PANi.^[36,37]

Estimation of Kinetic Parameters

Evaluation of the PANi multi-scan sweep rate voltammogram in figure 4 above indicate that the peak potentials for the emeraldine salt form of PANi (redox peak A') did not vary much with scan rate. The potential variation of this peak was $202 \pm$

14 PANi. For the first redox couple A/A', the cathodic to anodic peak current ratio (I_{pc} to I_{pa}) was 1.18 ± 0.16 . It means the PANi-ASA polymer exhibited reversibility at these scan rates. On repeated cycling of the PANi/ASA paste in the HCl electrolyte a thin green film appeared on the electrode. The surface concentration Γ^* (mol cm^{-2}) corresponding to this green film as estimated using the Brown Anson model^[38] was found to be 6.27×10^{-9} mol cm^{-2} .

The PANi-ASA voltammogram (Figure 4), shows that the peak potentials at peak 'A' shifts towards more negative values. The recorded potential range for this peak was 83 ± 27 mV. This indicates that a diffusion controlled charge transportation process is taking place along the polymer chain via an electron hopping process probably through the benzene rings. Plots of peak currents versus square root of scan rate for the peaks (A') are linear (Figure 4; $r^2 = 0.987$) and obey Randles-Sevcik relationship.^[38] The calculated charge transfer coefficients (D_e), was 6.41×10^{-7} cm^2/s . The value indicates that the movement of electrons along the polymer chain was averagely fast and agrees well with other diffusion coefficient values reported for doped PANi.^[1,20] The corresponding heterogeneous rate constant k^0 (cm/s) of 8.40×10^{-4} indicates the rate of electron exchange between the polymer chain and the electrode was

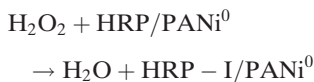
moderately fast. It means the ASA-doped PANi could be used as an electron mediator in the construction of amperometric biosensors.

The electrochemical behaviour of the ASA-doped PANi was also studied in phosphate buffer (pH 7.0). This study was necessitated by the fact that enzymes are pH sensitive and perform best within their physiological pH. Results in buffer showed (diagram not shown) that the PANi/ASA maintained its electroactivity even at this neutral pH indicating its ability to provide direct electrical communication between the enzymes and the electrode.

H₂O₂ Biosensors Based on Nanofibrillar ASA-doped PANi

The incorporation of horseradish peroxidase (HRP), a heme-containing glycoprotein onto the immobilization matrix, fine-tuned the sensor for hydrogen peroxide (H₂O₂) sensing. Previous reports have shown that HRP-catalysed reduction of the peroxides usually occurs in the presence of redox species, which are either electron donors or hydrogen donors.^[1] The catalytic reduction of hydrogen peroxide induces a two-electron oxidation of the ferric peroxidase (HRP Fe III –resting state) to an oxyferryl compound, HRP-I which is two oxidation equivalents above the resting

state. Through a two one-electron reduction steps the unstable HRP-I is converted to the stable form HRP Fe III through an intermediate hydroxyferryl state (HRP-II).^[1,39,40] In this biosensor format, the ASA-doped polyaniline will provide direct communication between the enzyme redox centre and the electrode. It is proposed that the reduced form of PANi/ASA will donate an electron to the HRP-I and another to the HRP-II states of the enzyme thus reducing it to the resting state.



Where PANi^{0/+} refer to the reduced and the oxidized forms of the polymer respectively. The PANi/ASA/HRP biosensor performance was studied at a low scan rate of 5 mV/s.

Figure 5 represents the PANi/HRP biosensor response to different concentration of 0.01 M H₂O₂.

The voltammograms depict the catalytic currents resulting from the coupling of the electro-oxidation of the ASA –doped polyaniline to the catalytic reduction of hydrogen peroxide. The currents produced

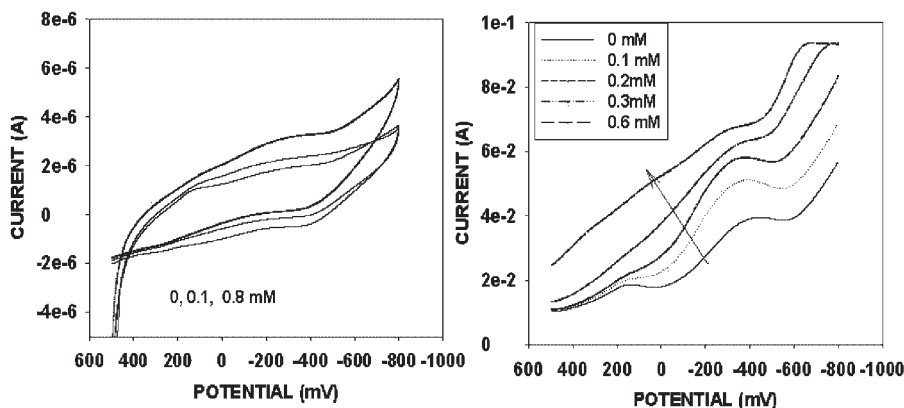


Figure 5.

Cyclic voltammetric responses of 0.0177 cm² Pt/pANI/ASA/2 mg mol⁻¹ horse radish peroxidase bioelectrode for hydrogen peroxide. Cyclic and differential pulse voltammograms (DPV) recorded under quiescent, anaerobic conditions in the potential ranges 600 to –1000 mV.

at any particular potential depend on the concentration of hydrogen peroxide present in the solution. That is the ASA-doped PANi is functioning as an electron-transfer mediator between the platinum electrode (transducer) and the HRP biomolecule. Clearly after the addition of a small amount of H_2O_2 , there is an enhancement of the cathodic peak at around -400 mV. The increase in the current of the peak at -400 mV demonstrates an effective electrocatalytic reduction of H_2O_2 on the platinum electrode. The on going sensor results were based on the assumptions that the HRP redox catalytic sites were non-diffusional.^[1] It was also assumed that the polymer-ASA-HRP sensors were thin homogeneous films in which the H_2O_2 reduction charge is propagated along the polymer chain by fast electron reactions involving the reduced and oxidized forms of the polymers.^[1]

This way, for a substrate limited kinetic case, the expression for the steady state

current (I), simplifies to the electrochemical Michaelis-Menten equation^[1,40] given by;

$$I = I_{\max}[\text{H}_2\text{O}_2]/([\text{H}_2\text{O}_2] + K'_M{}^{\text{app}}) \quad (3)$$

Where I is the observed catalytic current, I_{\max} is the maximum obtainable current for the biosensor, and $[\text{H}_2\text{O}_2]$ is the bulk solution concentration of hydrogen peroxide. Figure 6 represents the calibration curves for the various sensors response to different concentration of H_2O_2 as fitted into the Michaelis – Menten paradigm. The slope ($=I_{\max}/K'_M{}^{\text{app}}$) of the calibration curves were used to estimate the sensitivities of the biosensors. Results show that the PANi/ASA biosensor exhibited a sensitivity of 3.33×10^{-3} A/cm²/mM. The estimated $K'_M{}^{\text{app}}$ value for the sensor was $0.18 \text{ mM} \pm 0.01$. This $K'_M{}^{\text{app}}$ value represent the hydrogen peroxide concentration at which the sensor reaction kinetics changes from being first order to zero order.^[1,41,42] Also the maximum current density I_{\max} , value realized for this sensor

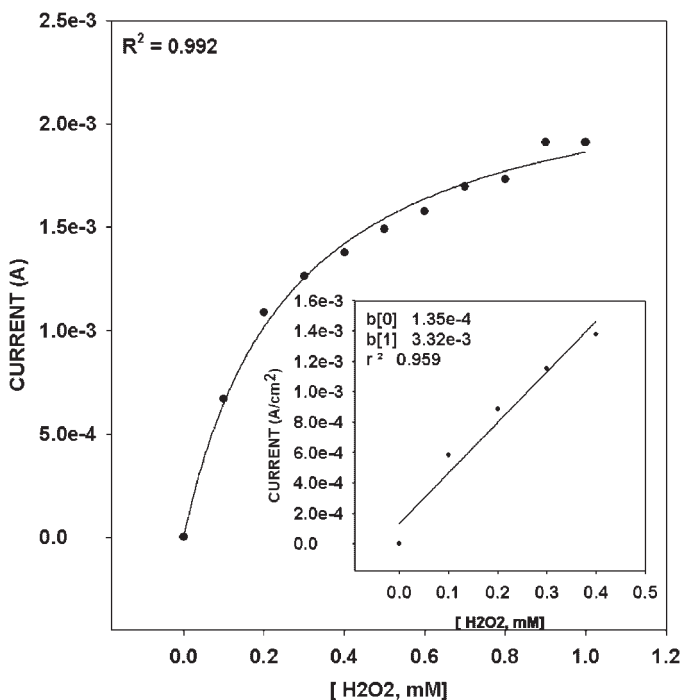


Figure 6.

Calibration curve for the polyaniline/horseradish peroxidase biosensor responses to different concentrations of $0.01 \text{ M H}_2\text{O}_2$. Inset, dynamic linear range of the sensor.

was $2.0 \times 10^{-3} \pm 0.03 \text{ A/cm}^2$. The values represent the current densities generated by the hydrogen peroxide concentration that brings about the switch in kinetic order. Thus the $K'M_{\text{app}}$ gives an indication of the enzyme-substrate system. This low $K'M_{\text{app}}$ for PANi-HRP complex is indicative of formation of a stable enzyme-substrate complex stability. It means the saturation of the enzyme active site occurs fast thus leading to a higher sensor response. The low $K'M_{\text{app}}$ value for the biosensor means higher sensitivity and the ability of the sensor to detect low substrate concentrations. The limit of detection (LOD) for a biosensor is normally three standard deviations the signal due to analyte divided by the sensitivity. The estimated LOD for the PANi/ASA biosensor was found to be $1.2 \times 10^{-2} \text{ mM}$ at an estimated signal to noise (S/N) ratio of 3. The biosensor exhibited a dynamic linear range of 0.012–0.45 mM. The linear range obtained here is larger than the 0.01–0.1 mM range obtained for a H_2O_2 based on poly-2-methylaniline-5-sulfonic acid (PMAS).^[43]

Amperometric Responses for the CYP 3A4/PANi/ASA Electrode

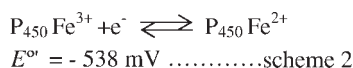
Cytochrome P450 3A4 is the major enzyme involved in the phase-1-biotransformation of xenobiotics. Cytochrome P450 3A4 is known to catalyse the N-demethylation of erythromycin, an antibiotic normally used to treat respiratory tract infections.^[22] Under normal physiological conditions, the demethylation reaction of CYP 3A4 follows the monooxygenation pathway in which NADPH acts as the source of the two electrons that drive the reaction^[44] as shown in the Scheme 1 below. Erythromycin contains two terminal methyl groups. It means that 4 electrons are needed for the complete demethylation process demanding a repeat of the scheme below.



In the construction of the CYP 3A4-based amperometric biosensor for erythromycin, the electrons for the monooxygenation were supplied by applying the appropriate potential through the Pt/PANi-ASA system. Figure 7(a) shows the CV of Pt-PANi/ (14.4 $\mu\text{mol/L}^{-1}$ solution) bioelectrode in 1 mL phosphate buffer saline (0.1 M, pH 7.4, 100 mM KCl) with or without erythromycin.

The Cyclic voltammetric responses of the PANi/ASA CYP 3A4 bioelectrode to different concentrations of erythromycin show one cathodic peak, ($E_{\text{pc}} = -538 \text{ mV}$). The cathodic peak current increased as the concentration of the erythromycin substrate increased. Differential pulse voltammetric responses (Figure 7(b)) of the PANi/ASA CYP electrode to different concentrations of erythromycin (0–3.75 μM) indicate there is a 286 mV potential shift towards more positive values. This indicates the presence of a catalytic reduction process coupled to an electrode transfer reaction at the electrode. This is also confirmed by the increase in cathodic current I_{pc} as the concentration of erythromycin increased up to 3.75 $\mu\text{mol/L}^{-1}$ erythromycin. A possible reaction scheme for the sensor-based N, N-demethylation of erythromycin is summarized in Figure 8.

Under anaerobic conditions the reduction of the ferric redox state in CYP 3A4



(Scheme 2) is coupled to the PANi^{0/+} oxidation/reduction as shown in Scheme 3 below;



The DPV results (Figure 7(b)) shows that the binding of erythromycin reduces the formal potential for the $\text{P}_{450} \text{Fe}^{3+/2+}$ by

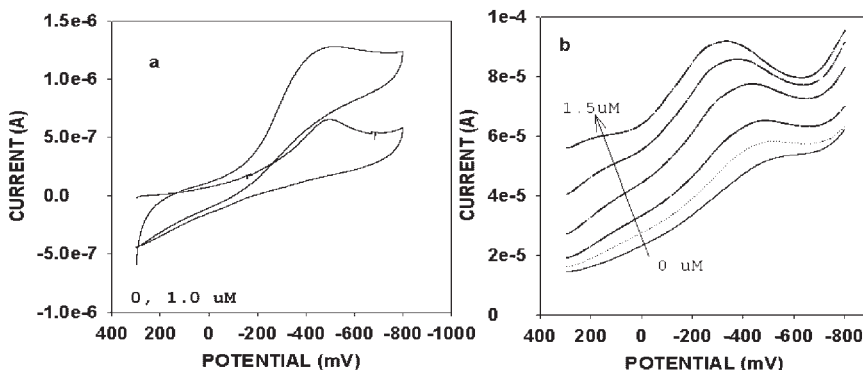
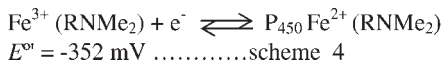


Figure 7.

Cyclic voltammetric responses of (0.0177 cm²) Platinum/14.4 μmol L⁻¹ CYP₄₅₀ 3A4 bioelectrode for erythromycin. Scan rate was 5 mV/s vs. Ag/AgCl at 20 °C.

286 mV at a substrate concentration of 3.75 μM/L⁻¹.



It has been shown that in this ferrous form (P₄₅₀Fe²⁺(RNMe₂)), the enzyme is an extremely efficient reducing agent and

combines with molecular oxygen to form a relatively stable oxygen-iron III complex, (P₄₅₀Fe³⁺O-O⁻).^[45] For the ongoing sensor, the phosphate buffer solution was not degassed after the addition of the substrate thus providing the oxygen necessary for this step. The acceptance of a second electron of this oxygen-iron III complex from the electrode through the PANI

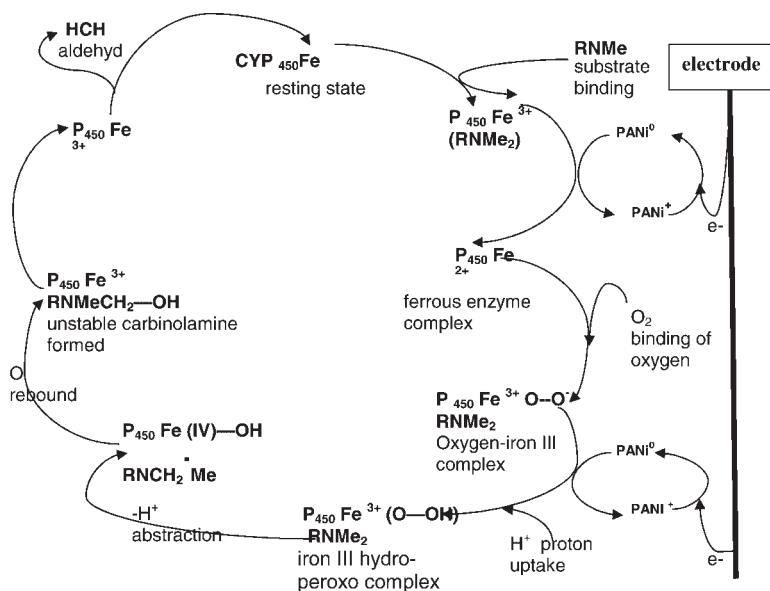


Figure 8.

Proposed scheme for the N, N-demethylation of erythromycin on a platinum/PANI/ASA, CYP 3A4 biosensor. Erythromycin consists of two N-CH₃ groups therefore the above cycle is repeated for complete demethylation.

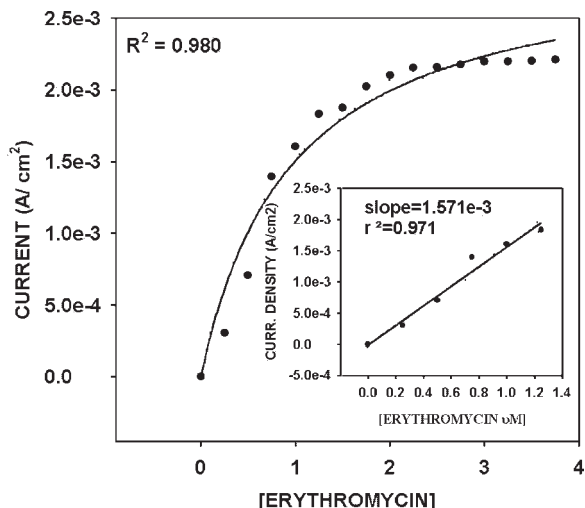


Figure 9.

Calibration curve for the polyaniline/Cytochrome P₄₅₀ 3A4 biosensor responses to different concentrations of 0.0005 M erythromycin. Inset: dynamic linear range of the sensor.

mediator, coupled with an uptake of a proton from the solvent, produces an iron III hydroperoxo compound (P₄₅₀Fe³⁺OOH) with an extremely high affinity for protons. It quickly abstracts a proton from one of the methyl groups in the erythromycin accompanied by a loss of a water molecule to form an iron IV hydroxo intermediate (P₄₅₀FeIV–OH). Through an oxygen rebound process, an unstable carbinolamine^[45,46,47] is formed and finally breaks down to HCHO and RNHCH₃. The cycle is then repeated for the complete demethylation of erythromycin.

The integrity of the PANi/CYP3A4 biosensor was evaluated through calculation of several biosensor parameters. Data points were fitted into the Michaelis-Menten equation to obtain a calibration curve (Figure 9). The apparent $K'M_{app}$ of the sensor for erythromycin was $0.8 \pm 0.1 \mu\text{mol/L}^{-1}$. The maximum current density I_{max} had a value of $(2.21 \pm 0.03) \times 10^{-3} \mu\text{A cm}^{-2}$ for the bioelectrode. The linear range of the biosensor has an upper limit of approximately $1.3 \mu\text{M}$ ($r^2 = 0.971$). The sensitivity of the biosensor representing the slope of the calibration graph is $1.57 \times 10^{-3} \mu\text{A cm}^{-2} (\mu\text{M})^{-1}$. The PANi

CYP 3A4 bioelectrode has a detection limit equal to $7.58 \times 10^{-2} \mu\text{M}$.

Conclusion

Polyaniline nanomaterials were successfully prepared. Spectroscopical and electrochemical characterization revealed that the materials were both conductive and electroactive. Scanning electron microscopy showed that the anthracene sulfonic acid surfactant dopant modulated the PANi nanocomposites into nanofibrillar morphology.

The horseradish and cytochrome P₄₅₀ 3A4 fabricated biosensors for the quantification of H₂O₂ and erythromycin respectively were high performing. It means the PANi/ASA materials acted as effective electron mediators providing direct electrical communication between the enzymes and the platinum electrode.

[1] E. I. Iwuoha, D. S. Villaverde, N. P. Garcia, M. R. Smyth, J. M. Pingarron, *Biosens. Bioelectron.* **1997**, 12, 49.

[2] M. G. Han, S. K. Cho, S. G. Oh, S. S. Im, *Synth. Met.* **2002**, 126, 53.

- [3] Z. Zhang, Z. Wei, L. Zhang, M. Wan, *Acta Materialia* **2005**, 53, 1373.
- [4] X. Luo, A. J. Killard, A. Morrin, M. R. Smyth, *Analytica Chimica Acta* **2006**, 575, 39.
- [5] W. Xue, K. Fang, H. Qiu, J. Li, W. Mao, *Synth. Met.* **2006**, 156, 506.
- [6] L.-M. Huang, T.-C. Wen, A. Gopalan, *Synth. Met.* **2002**, 130, 155.
- [7] Y. Wei, W. W. Focke, G. E. Wnek, A. Ray, A. G. MacDiarmid, *J. Phys. Chem.* **1989**, 93, 495.
- [8] A. Gökb, B. Sari, M. Talu, *Synth. Met.* **2004**, 142, 41.
- [9] M. Leclerc, J. Guay, L. H. Dao, *Macromolecules* **1989**, 22, 641.
- [10] W. Y. Zheng, K. Levon, J. Laasko, J. E. Osterholm, *Macromolecules* **1994**, 27, 77, 54.
- [11] S. S. Pandey, S. Annapoomi, B. D. Malhotra, *Macromolecules* **1993**, 26, 3190.
- [12] A. Malinauskas, *Polymer* **2001**, 42, 3957.
- [13] C. DeArmit, S. P. Armes, *Langmuir* **1998**, 9, 652.
- [14] M. E. Levya, G. M. O. Barra, B. G. Soares, *Synth. Met.* **2001**, 123, 443.
- [15] Z. Wei, M. Wan, *Advanced Materials* **2002**, 14, 18, 1314.
- [16] Z. Wei, Z. Zhang, M. Wan, *Langmuir* **2000**, 18, 917.
- [17] L. Zhang, M. Wan, *Thin Solid Films* **2005**, 477, 24.
- [18] A. Morrin, F. Wilbeer, O. Ngamna, S. E. Moulton, A. J. Killard, G. G. Wallace, M. R. Smyth, *Electrochem. Communi.* **2005**, 7, 317.
- [19] G. Kathleen, A. J. Killard, C. J. Hanson, A. A. Cafolla, M. R. Smyth, *Talanta* **2006**, 68, 1591.
- [20] N. G. R. Mathebe, A. Morrin, E. I. Iwuoha, *Talanta* **2004** 64, 115.
- [21] C. M. Faulkner, H. L. Cox, J. C. Williamson, *Clinical Infectious Diseases* **2005**, 40, 997.
- [22] P. L. Albert, D. L. Kaminiski, A. Rasmussen, *Toxicology* **1995**, 104.
- [23] <http://en.wikipedia.org/wiki/Erythromycin>
- [24] X. Zhang, S. K. Manohar, *Chem. Commun.* **2004**, 2360.
- [25] B.-K. Kim, Y. H. Kim, W. Keehoon, C. Hyunju, C. Younming, K.-J. Kong, B. W. Rhyu, J.-J. Kim, J.-O. Lee, *Nanotechnology* **2005**, 16, 1117.
- [26] M. R. Fernandes, J. R. Garcia, M. S. Schultz, F. C. Nart, *Thin Solid Films* **2005**, 474, 279.
- [27] L. Zhang, M. Wan, *Nanotech.* **2002**, 13, 750.
- [28] A. Malinauskas, R. Holze, *Synth. Met.* **1998**, 97, 31.
- [29] E. M. Guerra, C. A. Brunello, C. F. O. Graeff, H. P. Oliveira, *J. Solid State Electrochem.* **2002**, 168, 134.
- [30] Y. H. Geng, Z. C. Sun, J. Li, X. B. Jing, X. H. Wang, F. S. Wang, *Polymer* **1999**, 46, 5723.
- [31] A. Dey, S. De, A. De, S. K. De, *Nanotechnology* **2004**, 1277.
- [32] A. Mirmohseni, G. G. Wallace, *Polymer* **2003**, 44, 3523.
- [33] Y. Wei, W. W. Focke, G. E. Wnek, A. Ray, A. G. MacDiarmid, *J. Phys. Chem.* **1989**, 93, 495.
- [34] L.-M. Huang, C.-H. Chen, T.-C. Wen, A. Gopalan, *Electrochimica Acta* **2006**, 51, 2756.
- [35] B. Valter, M. K. Ram, C. Nicolini, *Langmuir* **2002**, 18, 1535.
- [36] T. Lindfors, A. Ivaska, *J. Electroanal. Chem.* **2002**, 531, 43.
- [37] S. E. Moulton, P. C. Innis, L. A. P. Kane Maguire, O. Ngamna, G. G. Wallace, *Current Applied Physics* **2004**, 4, 402.
- [38] A. J. Bard, L. R. Faulkner, "Electrochemical Methods. Fundamentals and Applications", 2nd edition, John Wiley & Sons Inc., New York, NY **2001**.
- [39] L. Komsijska, T. Tsacheva, V. Tsakova, *Thin Solid Film* **2005**, 493, 88.
- [40] I. E. Iwuoha, L. Ingrid, M. Enda, M. R. Smyth, Ó. F. Cláran, *Anal. Chem.* **1997**, 69, 1674.
- [41] E. I. Iwuoha, O. Adeyoju, E. Dempsey, M. R. Smyth, J. Liu, J. Wang, *Biosens. Bioelectron.* **1995**, 10, 661.
- [42] M. Pravda, C. M. Jungar, E. I. Iwuoha, M. R. Smyth, K. Vytras, A. Ivaska, *Anal. Chimica Acta* **1995**, 304, 127.
- [43] O. Ngamna, A. Morrin, S. E. Moulton, A. J. Killard, M. R. Smyth, G. G. Wallace, *Synth. Met.*, 2005 153, 185.
- [44] E. I. Iwuoha, A. Wilson, M. Howel, N. G. R. Mathebe, K. Montane-Jaime, D. Narinesingh, A. Guiseppe-Elie, *Analytical letters* **2004**, 37, 5, 000–000.
- [45] B. Meunier, S. P. de Visse, S. Shaik, *Chem. Rev.* **2004**, 104, 3947.
- [46] G. T. Miwa, J. S. Walsh, *J. Biological Chemistry* **1983**, 258, 14445.
- [47] F. P. Guengerich, C.-H. Yun, T. L. Macdonald, *J. Biological Chemistry* **1996**, 271, 27321.